

# Vesicular Stomatitis Virus Expressing Tumor Suppressor p53 Is a Highly Attenuated, Potent Oncolytic Agent<sup>∇</sup>

Joshua F. Heiber and Glen N. Barber\*

Departments of Cell Biology and Microbiology and Immunology and the Sylvester Comprehensive Cancer Center, University of Miami Miller School of Medicine, Miami, Florida 33136

Received 14 June 2011/Accepted 17 July 2011

**Vesicular stomatitis virus (VSV), a negative-strand RNA rhabdovirus, preferentially replicates in and eradicates transformed versus nontransformed cells and is thus being considered for use as a potential anticancer treatment. The genetic malleability of VSV also affords an opportunity to develop more potent agents that exhibit increased therapeutic activity. The tumor suppressor p53 has been shown to exert potent antitumor properties, which may in part involve stimulating host innate immune responses to malignancies. To evaluate whether VSV expressing p53 exhibited enhanced oncolytic action, the murine p53 (mp53) gene was incorporated into recombinant VSVs with or without a functional viral M gene-encoded protein that could either block (VSV-mp53) or enable [VSV-M(mut)-mp53] host mRNA export following infection of susceptible cells. Our results indicated that VSV-mp53 and VSV-M(mut)-mp53 expressed high levels of functional p53 and retained the ability to lyse transformed versus normal cells. In addition, we observed that VSV-ΔM-mp53 was extremely attenuated *in vivo* due to p53 activating innate immune genes, such as type I interferon (IFN). Significantly, immunocompetent animals with metastatic mammary adenocarcinoma exhibited increased survival following treatment with a single inoculation of VSV-ΔM-mp53, the mechanisms of which involved enhanced CD49b<sup>+</sup> NK and tumor-specific CD8<sup>+</sup> T cell responses. Our data indicate that VSV incorporating p53 could provide a safe, effective strategy for the design of VSV oncolytic therapeutics and VSV-based vaccines.**

Cancer is a leading cause of morbidity and mortality worldwide, necessitating the continuing development of new therapeutics to combat the disease. However, current treatment modalities, such as radiation and chemotherapy, can lead to debilitating side effects, as well as the selection of more aggressive malignant disease (63). The use of viral agents is a further option presently being considered for the treatment of cancer. This strategy is based on observations that numerous types of viruses preferentially replicate in cancer cells versus normal cells, since the former type appear to have acquired defects in innate immune signaling processes that would usually prevent efficient replication (5). The ability to genetically manipulate many of these viral agents also affords an opportunity to increase their therapeutic efficacy by stimulating antitumor immune responses or increasing bystander effects (35, 44, 45). Viruses being considered for oncolytic agents include measles virus, adenovirus, herpes simplex virus, and vesicular stomatitis virus (VSV) (48).

VSV is an 11-kb negative-strand RNA virus of the family *Rhabdoviridae*. It is nontransforming, has a low seroprevalence, causes minimal morbidity and mortality in humans, and is genetically malleable, allowing transgenes of interest to be incorporated into the genome to generate recombinant VSV (rVSV). For example, it has been demonstrated that rVSVs designed to express cellular genes that modulate immunity, such as beta interferon (IFN-β) genes, exhibit effective onco-

lytic activity with increased antitumor immune responses (44, 49). Genetically modifying the VSV genome itself is also possible and has proved useful in anticancer strategies. For example, VSVs harboring a mutation of the matrix (M) gene that renders the protein incapable of blocking mRNA export from the nucleus enabled the stimulation of robust innate immune responses following the infection of cancer cells that were characterized by an increase in IFN-β and interferon-stimulated gene (ISG) production (59, 61). The triggering of innate immune responses is essential to facilitate upregulation of antigen-presenting machinery, stimulate NK cell activity, and induce anticancer cytokines.

Recently, it was reported that the p53 tumor suppressor protein could inhibit tumor formation through mechanisms that involved the stimulation of innate immunity, including cross talk with the IFN system (53, 55, 62). p53 is a well-documented regulator of many ubiquitous cellular processes and is mutated or deleted in more than 50% of all cancers. Further, p53 is known to potently modulate signal transduction pathways, including cellular senescence and cell cycle pathways (29). Additionally, p53 can affect the expression of several transcriptional gene expression profiles, including those involving DNA repair and apoptosis (26, 29). It has also previously been observed that reactivation of p53 in murine tumor models can increase innate immune antitumor activity (62). Given this, we considered whether the incorporation of p53 into VSV would increase host antitumor innate immune responses that, in conjunction with direct oncolytic activity, could facilitate tumor clearance. We therefore incorporated the murine p53 (mp53) gene into VSV, hypothesizing that this could yield a more effective cancer therapeutic agent.

In addition to generating a VSV p53-expressing vector with

\* Corresponding author. Mailing address: Department of Cell Biology, University of Miami Miller School of Medicine, Room 510 Papanicolaou Bldg., 1550 NW 10th Ave. (M710), Miami, FL 33136. Phone: (305) 243-5914. Fax: (305) 243-5885. E-mail: gbarber@med.miami.edu.

<sup>∇</sup> Published ahead of print on 3 August 2011.

normal viral genes, we also generated a recombinant VSV expressing p53 with a defective M protein: amino acids 52 to 54 of the M protein were mutated from DTY to AAA. This mutation prevents the M protein from binding to the Rae1-Nup98 mRNA export complex and allows cells infected with VSV-M(mut) to efficiently export mRNA from the nucleus, such as type I IFN and other virus- or p53-activated host genes (16, 59, 61). This facilitates the initiation of stronger innate immune responses, which can facilitate antitumor immunity in tumor cells, as well as prevent viral infection of cells with intact innate immune signaling pathways.

## MATERIALS AND METHODS

**Cells and transfection.** C57BL/6 and 129/B6 mouse embryonic fibroblasts (MEFs) were maintained in Dulbecco's modified Eagle's medium (DMEM) supplemented with 10% fetal bovine serum (FBS), 5% penicillin-streptomycin, and 1% nonessential amino acids. B16(F10) cells were maintained in DMEM supplemented with 10% FBS, 5% penicillin-streptomycin, and 1.5 g/liter sodium bicarbonate. BHK cells were maintained in DMEM supplemented with 10% FBS and 5% penicillin-streptomycin; TS/A and TS/A-luc cells were maintained in RPMI 1640 supplemented with 10% FBS, 5% penicillin-streptomycin, and 10 mg/ml puromycin for TS/A-luc. C57BL/6 MEFs were transfected using Lipofectamine LTX and Plus reagents (Invitrogen); all other cell lines were transfected using Lipofectamine 2000 (Invitrogen) according to the manufacturer's protocol.

**Generation of VSV-mp53 and VSV-DM-mp53.** In order to obtain the mp53 cDNA, PCR was performed using Pfx super mix (Invitrogen) and the oligonucleotides FWD (5'-TTATGTCGACATGACTGCCATGGAGGAGTC-3') and REV (5'-GCTAGCAGCCCTGAAGTCATA-3') with the pORF-mp53 construct as a template (Invitrogen). The PCR product was then ligated into pCR-Blunt II Topo (Invitrogen), and the sequence was verified. mp53 was then digested using SalI and NheI restriction enzymes (NEB) and gel purified. mp53 was then cloned into the XhoI and NheI sites of VSV-XN2 and VSV-M(mut). VSV-M(mut) was generated by mutating amino acids 52 to 54 of the M protein from DTY to AAA using a site-directed mutagenesis kit (Stratagene) with the following oligonucleotides: for amino acid 52 D to A, FWD, 5' GGAGTTGAC GAGATGGCCACCTATGATCCGAATC, and REV, 5' GATTCCGGATCATA GTTGCCATCTCGTCAACTCC; for amino acid 53 T to A, FWD, 5' GGA GTTGACGAGATGGACGCCACCTATGATCCGAATC, and REV, 5' GATT CGGATCATAGGTGGCGTCCATCTCGTCAACTCC; and for amino acid 54 Y to A, FWD, 5' TTTGGAGTTGACGAGATGGACACCGCTGATCCGAAT CAATTAAG, and REV, 5' CTTAATTGATTCGGATCAGCGGTGTCCATC TCGTCAACTCAAAA. Virus was then grown using a virus recovery protocol described previously (34). Purification and concentration were achieved using sucrose centrifugation. Viral titers were obtained using the standard plaque assay.

**Virus infections.** MEFs and TS/A and B16(F10) cells were seeded in 6 or 12-well plates and grown to 70% confluence. After washing with 1× phosphate-buffered saline (PBS), the cells were infected with rVSVs at the indicated multiplicity of infection (MOI), which was calculated as follows: (number of cells × MOI)/titer = ml virus needed. The cells were incubated with virus for 1 h at 37°C in serum-free DMEM with rocking every 15 min. The cells were washed with PBS twice, and complete medium was added to the cells.

**Cell viability.** C57BL/6 MEFs and TS/A and B16(F10) cells were grown to 70% confluence in 12-well plates. The cells were then infected as described above at the indicated MOIs. After incubation for 6, 12, 24, and 48 h, cells were collected, washed with PBS twice, and suspended in annexin V buffer (BD; 51-66121E). The cells were then stained using annexin V-eFluor 450 (1 μg/ml; eBioscience) and propidium iodide (1 μg) and then used for flow cytometry. Cells were considered dead when they shifted from being annexin V single positive (early apoptotic) to annexin V-propidium iodide double positive (late apoptotic).

**Western blotting.** Infected cells were collected and lysed in radioimmunoprecipitation assay (RIPA) buffer containing protease and phosphatase inhibitors. Protein concentrations were determined using Coomassie Plus Protein Assay Reagent (Thermo; 1856210), and the optical density (OD) was read at 595 nm. Equal amounts of protein were subjected to SDS-PAGE, transferred onto a polyvinylidene difluoride (PVDF) membrane, and blocked using 5% milk in PBS-Tween (0.1% Tween 20). The membranes were then immunoblotted using antibodies against p53 (Santa Cruz; SC-99), p53 phosphorylated at serines 18 and 389 (Cell Signaling; 9284 and 9281), and VSV-G (Sigma; V5507). The membranes were probed with a secondary antibody, goat anti-mouse, goat anti-rabbit,

or donkey anti-goat (Santa Cruz), at 1:5,000. The image was resolved using chemiluminescence (Super Signal) and captured by autoradiography (Kodak Film).

**p53 luciferase assay.** Firefly p53-luc (Clontech; 250 ng) and *Renilla* pRLTK (50 ng) were transfected as described previously into 70% confluent C57BL/6 MEFs and TS/A and B16(F10) cells grown in 12-well plates 4 h prior to infection. The cells were then infected as described above at the desired MOI. After 24 h, the cells were lysed using 1× luciferase cell culture lysis reagent (CCLR), and luciferase assays were performed using a Luciferase Assay System and a *Renilla* Assay System (Promega).

**p53 DNA microarray.** C57BL/6 MEFs and TS/A cells were grown to 70% confluence in 6-well plates and infected as described previously at the indicated MOI. After 8 h incubation, total RNA was collected using an Array-Grade Total RNA Isolation Kit (SA Biosciences). cDNA and biotin-labeled cRNA were then generated using TrueLabeling-AMP 2.0 (SA Biosciences). The labeled cRNA was then hybridized to an Oligo GEArray DNA Microarray (OMM-027) and resolved using chemiluminescent detection and autoradiograph capture.

**Mouse studies.** Female BALB/c mice (6 to 8 weeks old) were acquired from Jackson Laboratory. Female BALB/c athymic nude (CAN.Cg-Foxn1<sup>tm</sup>/Cr) mice were acquired from Charles River. All mice were housed under pathogen-free conditions.

**Toxicity.** Female BALB/c ( $n = 7$ ) or nude ( $n = 5$ ) mice were injected with VSV intravenously (i.v.) in 100 μl PBS in the tail vein or in 10 μl PBS intranasally (i.n.). The mice were then monitored for survival. Additionally, mice were sacrificed if they displayed gross morbidity or if they developed hind limb paralysis.

**Tumor studies.** BALB/c ( $n = 7$ ) or nude ( $n = 5$ ) mice were injected with  $1 \times 10^5$  TS/A-luc cells i.v. Three days later, the mice were injected with  $5 \times 10^7$  or  $5 \times 10^8$  PFU of rVSV. The survival of the mice was monitored daily. The surviving mice were rechallenged with  $2 \times 10^5$  TS/A-luc cells and monitored daily for survival.

**ELISPOT.** We followed the protocol for the enzyme-linked immunospot (ELISPOT) assay as previously described in detail (R&D) (1). Female BALB/c mice ( $n = 5$ ) were injected i.v. in the tail vein with  $1 \times 10^5$  TS/A-luc cells. Three days later, the mice were infected with  $5 \times 10^7$  PFU of the indicated rVSV i.v., and 10 days postinfection, the mice were sacrificed and the spleens were removed. TS/A-luc cells treated with mitomycin C (25 μg/ml) were used as the target. The plates were analyzed the following day using an ELISPOT reader.

**Multiplex ELISA and flow cytometry.** Female BALB/c ( $n = 6$ ) mice were infected with  $5 \times 10^7$  PFU rVSV i.v. Twenty-four ( $n = 3$ ) and 96 ( $n = 3$ ) hours postinfection, the sera, spleens, and thymuses were collected. The sera were stored at  $-80^\circ\text{C}$  and used for multiplex enzyme-linked immunosorbent assay (ELISA) (Millipore). The sera were incubated overnight at  $4^\circ\text{C}$  with agitation with a mix of antibody-coated beads. The next day, samples were incubated with detection antibodies for 1 h at room temperature and run on a Luminex 100 machine. The spleens and thymuses were passed through a  $0.2\text{-}\mu\text{m}$  mesh, and cells were recovered in 3 ml of RPMI 1640. The cells were then centrifuged at 1,400 rpm, and red blood cells were lysed using 1 ml of ACK buffer (red blood cell lysis buffer [0.15 M  $\text{NH}_4\text{Cl}$ , 1 M  $\text{KHCO}_3$ , 0.1 mM  $\text{Na}_2\text{EDTA}$ ]) for 5 min, centrifuged again, and washed with 1× PBS. The cells were counted, and two groups of  $1 \times 10^6$  cells were stained for 4-color flow cytometry using CD4-phycoerythrin (PE) (BD 557308), CD8-peridinin chlorophyll protein (PerCP) (BD 553036), B220-fluorescein isothiocyanate (FITC) (BD 553088), CD49b-allophycocyanin (APC) (eBioscience 17-5971-81), CD11c-FITC (BD 553801), CD11b-APC (BD553312), F4/80-PE (eBioscience 12-4801-80), or major histocompatibility complex class II (MHC-II)-eFlour450 (eBioscience 48-5321-80) on ice in darkness for 20 min. The cells were then washed once with PBS and fixed with 1 to 4% paraformaldehyde and stored in the dark at  $4^\circ\text{C}$  until samples were run on flow cytometry (BD-LSRI).

**IFN-β ELISA.** BALB/c mice ( $n = 3$ ) were mock infected or infected with  $5 \times 10^7$  PFU rVSV. Six hours postinfection, blood was collected by submandibular bleeding. The blood was then incubated for 1 h at  $4^\circ\text{C}$  and centrifuged at 13,000 rpm in order collect serum. Samples were diluted 1:50 and assessed by IFN-β ELISA (PBL Interferonsource).

**In vivo imaging of mice.** Mice were imaged as previously described (58).

**Statistics.** All statistical analysis was performed using GraphPad Prism 5.

## RESULTS

**Generation of oncolytic VSV-M(mut)-mp53 and VSV-mp53.** To determine whether novel VSVs expressing p53 have an improved ability to modulate innate and adaptive immune

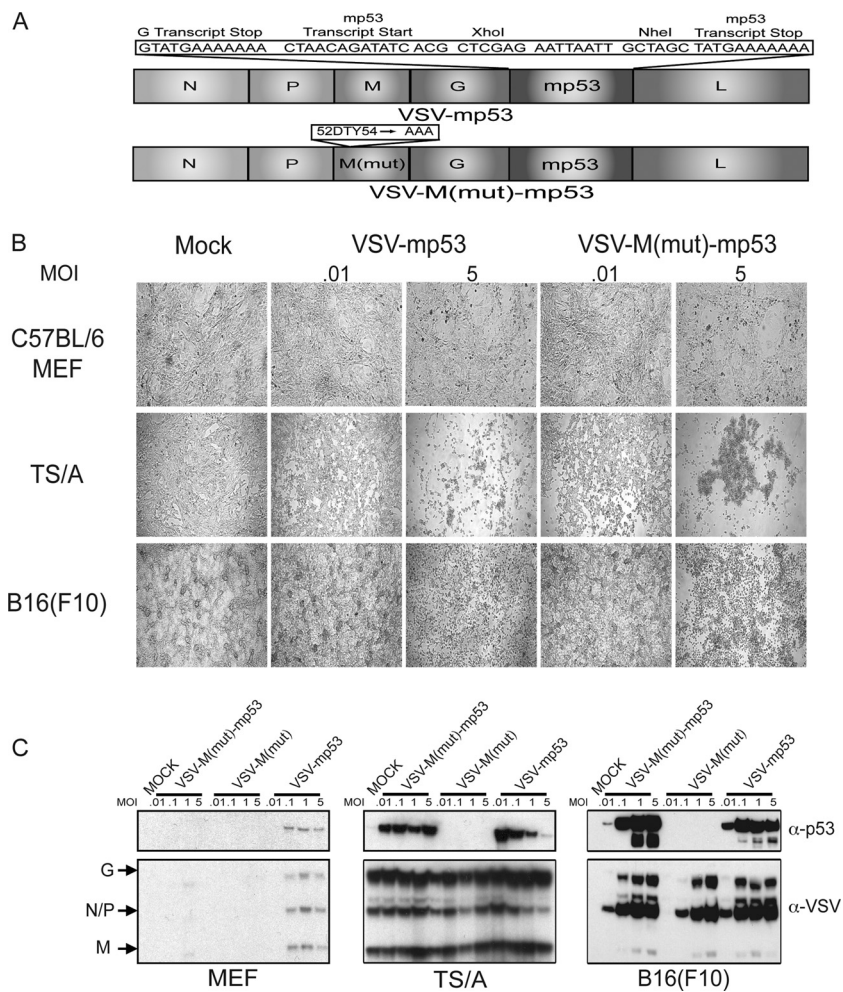


FIG. 1. VSV-M(mut)-mp53 and VSV-mp53 retain oncolytic ability and express mp53. (A) Schematic representation of VSV p53 constructs. (B) Bright-field microscopy of VSV-M(mut)-mp53- and VSV-mp53-infected cells at MOIs of 0.01 and 5 24 h postinfection. Mock, mock infection. (C) Immunoblot analysis for VSV and mp53 protein expression in infected C57BL/6 MEFs and TS/A or B16(F10) cells infected at MOIs of 0.01, 0.1, 1, and 5 24 h postinfection.

responses that may result in increased antitumor efficacy and safety *in vivo*, the mp53 gene was cloned between the G and L proteins of VSV (VSV-XN2). As an additional experiment, murine p53 was similarly cloned into VSV harboring a mutation in the M protein [VSV-M(mut)] so that the resultant virus could not block host mRNA export, including innate immune-related transcripts that could conceivably be triggered by heterologous p53 activity. The resulting plasmids were then used to recover functional viral particles as previously described (34) (Fig. 1A). To verify that the resulting VSV-M(mut)-m and VSV-mp53 retained oncolytic specificity, normal C57BL/6 MEFs or tumor [murine mammary adenocarcinoma TS/A or murine melanoma B16(F10)] cells were infected at an MOI of 0.01, 0.1, 1, and 5 for 24 h. Cytopathic effect (CPE) was observed using bright-field microscopy (Fig. 1B). Our results indicated that only the TS/A and B16(F10) tumor lines exhibited the characteristics of infection as manifested by CPE, in contrast to the normal MEFs (5). The MEFs and tumor cells were then lysed and examined by immunoblotting to confirm the expression of the mp53 transgene (Fig. 1C). This analysis indi-

cated that both VSV-mp53 and VSV-M(mut)-mp53 efficiently expressed the mp53 transgene in tumor cell lines [TS/A and B16(F10)] permissive for VSV replication. These data emphasize that VSV can efficiently express the p53 gene and that normal MEFs do not support robust viral replication.

To further evaluate whether VSV-mp53 or VSV-M(mut)-mp53 retained the ability to replicate efficiently in and kill transformed cells, normal MEFs and TS/A or B16(F10) cells were infected with the above-mentioned rVSVs. The results indicated that VSV-mp53 and VSV-M(mut)-mp53, as well as control VSV-green fluorescent protein (GFP) and VSV-M(mut)-GFP, effectively killed TS/A and B16(F10) cells and replicated to similar titers within 24 h (Fig. 2A to C). Importantly, VSV-mp53 and VSV-M(mut)-mp53 retained oncolytic specificity, since MEFs remained largely unaffected by rVSV infection (Fig. 2A) (5, 6). Indeed, MEFs generated 2 to 3 log units less virus as measured 24 h postinfection than TS/A or B16(F10) cells (Fig. 2D to F). Moreover, viruses expressing p53 replicated even less in MEFs than control VSV-GFP. Our analysis indicates that MEFs are not robustly permissive to

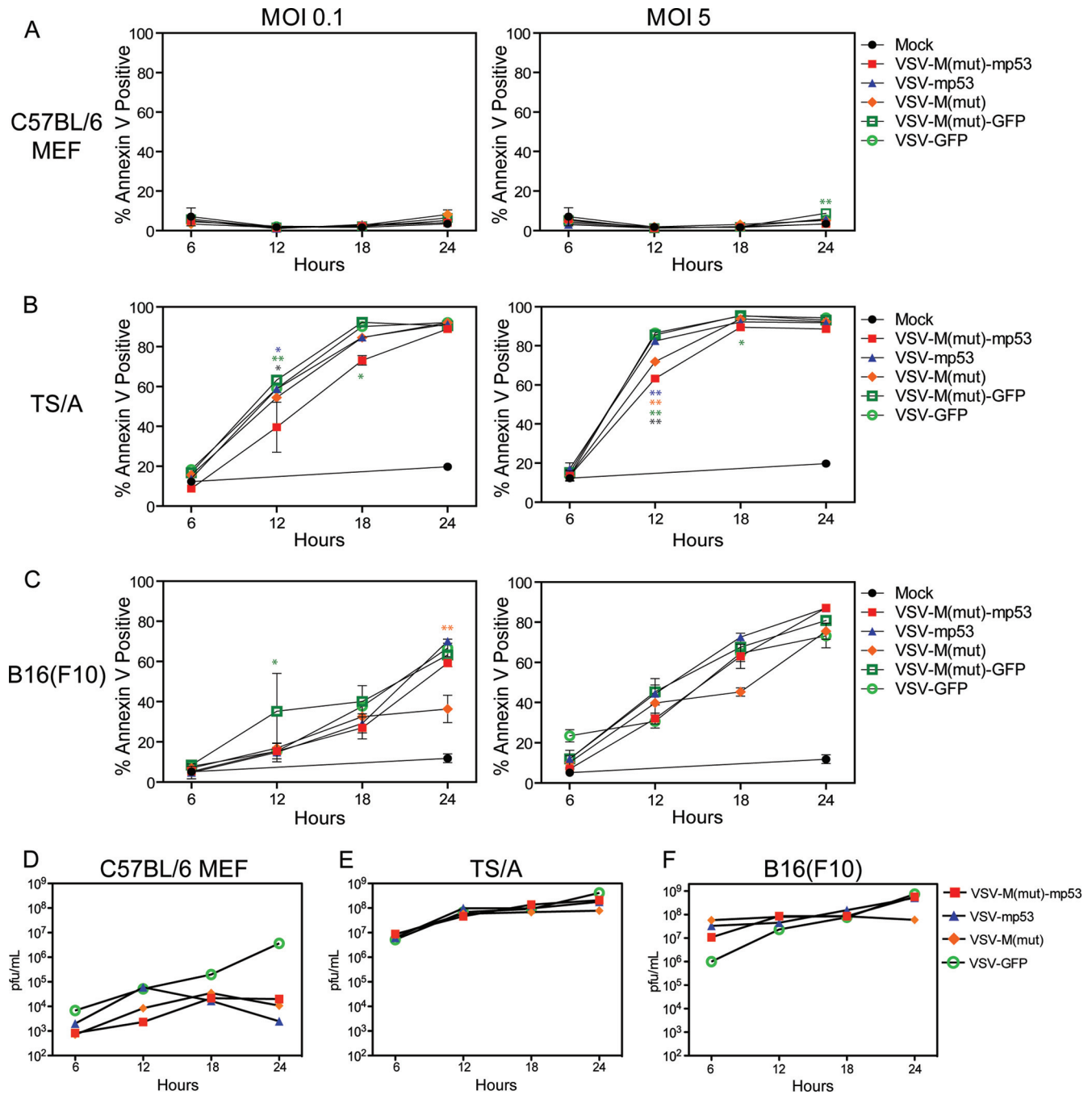


FIG. 2. VSV-M(mut)-mp53 and VSV-mp53 replication *in vitro*. C57BL/6 MEFs and TS/A or B16(F10) cells were infected with rVSVs at an MOI of 0.1, 1, or 5. Cells and supernatants were collected 6, 12, 18, and 24 h postinfection. (A, B, and C) Cell death at each time point as determined by annexin V-propidium iodide staining. (D, E, and F) Supernatants were analyzed by the standard plaque assay to determine the replication of rVSVs. (Two-way analysis of variance [ANOVA]/Bonferroni posttest: \*,  $P < 0.001$ ; \*\*,  $P < 0.0001$ ; blue asterisks, VSV-M(mut)-mp53 versus VSV-mp53; orange asterisks, VSV-M(mut)-mp53 versus VSV-ΔM; green asterisks, VSV-M(mut)-mp53 versus VSV-M(mut)-GFP; black asterisks, VSV-M(mut)-mp53 versus VSV-GFP). The error bars indicate standard deviations.

VSV infection compared to transformed TS/A and B16 cells (59). This may be due to MEFs having intact innate immune pathways that could combat infection. These data clearly suggest that insertion of mp53 into either the XN2 or M(mut) background does not inhibit the replicative or oncolytic abilities of these viruses *in vitro*.

**Expressed mp53 is phosphorylated and activates transcription of target genes.** It is well known that mp53 undergoes a variety of posttranslational modifications, such as phosphorylation, ubiquitination, sumoylation, acetylation, and neddylation, in order to regulate its activity (9, 33, 38, 52). For example, murine p53 can be activated by phosphorylation on serine

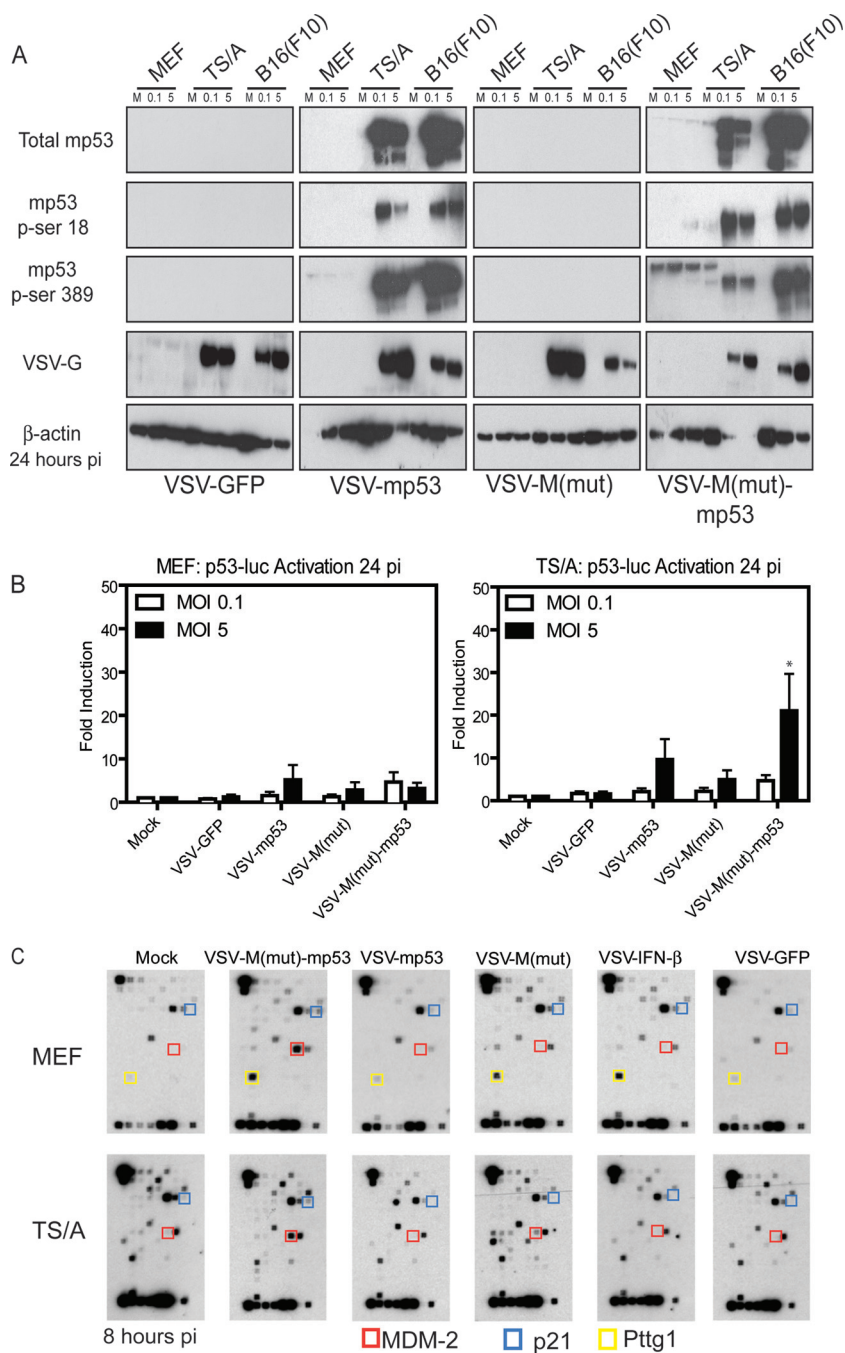


FIG. 3. Expressed mp53 is functional. (A) C57BL/6 MEFs and TS/A or B16(F10) cells were infected with rVSV at MOIs of 0.1 and 5. The cells were lysed 24 h postinfection (pi) and used for immunoblot analysis. (B) C57BL/6 MEFs or TS/A cells were transfected with a p53 luciferase reporter and then infected at an MOI of 0.1 or 5. Luciferase levels were assessed 24 h postinfection. (\*,  $P = 0.0366$ ; one-way ANOVA.) The error bars indicate standard deviations. (C) C57BL/6 MEFs or TS/A cells were infected at an MOI of 10 or 1, respectively, and mp53 target gene mRNA expression was determined.

18. This event is carried out by DNA-dependent protein kinase (DNA-PK) in response to cellular stress, which causes dissociation of p53 from its negative regulator, MDM-2 (an E3 ubiquitin ligase), and allows p53 stabilization (36, 52). In addition, serine 389 can be phosphorylated, which induces the p53 oligomerization necessary for DNA binding and transcription activation activities (13, 27). To evaluate whether mp53

expressed by VSV-mp53 or VSV-M(mut)-mp53 was active, mock- or rVSV-infected cell lysates were immunoblotted using phosphorylation-specific murine p53 antibodies. This analysis confirmed efficient expression of the mp53 transgene that correlated well with the ability of rVSV to preferentially replicate in transformed cells (Fig. 3A). Additionally, membranes were probed with phosphoserine 18- or 389-specific antibodies to

determine if virus-expressed mp53 is phosphorylated on serine residues necessary for stabilization and transcriptional activation (Fig. 3A). Confirmation that mp53 is indeed phosphorylated on serines 18 and 389 provided initial evidence that mp53 produced during viral replication is capable of being activated and may be able to initiate the transcription of target genes. Next, to ascertain if VSV-expressed phosphorylated mp53 is transcriptionally active, we performed a p53 luciferase reporter assay (Fig. 3B). Essentially, VSV-mp53 and VSV-M(mut)-mp53 were used to infect normal or tumor cells transiently expressing a luciferase reporter gene under the control of a p53 promoter element. This analysis indicated that permissive TS/A cells exhibited an increase in luciferase expression compared to normal MEFs following infection with VSVs expressing p53. This is likely due to TS/A cells supporting high levels of viral replication. However, MEFs also exhibited some luciferase expression after infection with rVSVs expressing p53, suggesting that modest amounts of heterologous p53 may be being produced in these cells, albeit at very low levels. However, it has been shown that VSV infection can also modestly induce the activation of mp53 through a cross talk mechanism involving the type I IFN response (55). An important observation from this experiment was that luciferase expression was higher in cells infected with VSV-M(mut)-mp53, presumably because more luciferase mRNA was able to escape from the nucleus for translation (Fig. 3B) (15). To extend this examination further, the ability of virus-encoded mp53 to activate transcription was additionally assessed using a p53 microarray harboring 112 p53-inducible genes (Fig. 3C). MEFs and TS/A cells were infected at an MOI of 10 or 1, respectively, for 1 h and lysed 8 h postinfection to retrieve cellular mRNA. The result indicated that infection with VSV-M(mut)-mp53 induced the robust production of the known p53-inducible MDM-2 (red boxes) and p21 (blue boxes) genes (Fig. 3C). Presumably, most of the other genes on the panel were not detected, since p53 may only weakly regulate these genes. One gene, encoding PTTG1 (pituitary tumor-transforming 1; yellow boxes) was observed to be induced in normal MEFs infected with VSV-M(mut) or VSV-IFN- $\beta$ , possibly because it has interferon-inducible transcription sites in its promoter region. These data highlight the potential advantage of using the VSVs with a defective matrix (M) protein, since MDM-2 and p21 mRNA induction were only robustly observed in cells infected with VSV-M(mut)-mp53, which cannot block host cell mRNA export. Additionally, these data confirm that virus-expressed murine p53 especially from VSV-M(mut), not only is appropriately posttranslationally modified, at least by phosphorylation on serines 18 and 389, but is transcriptionally active.

**VSV-M(mut)-mp53 is highly attenuated in BALB/c mice.** To start to evaluate the *in vivo* effects of VSV- $\Delta$ M-mp53, we carried out preliminary toxicity assays using murine models. BALB/c mice ( $n = 7$ ) were infected i.v. with increasing doses of  $1 \times 10^8$  to  $1 \times 10^9$  PFU of VSV-M(mut)-mp53, VSV-mp53, VSV-M(mut)-GFP, VSV-GFP, or VSV-IFN- $\beta$  (Table 1). Mice infected with VSV-GFP exhibited toxicity at doses of  $1 \times 10^8$  to  $5 \times 10^8$ . In contrast, VSV-mp53, VSV-M(mut), and VSV-M(mut)-GFP appeared more attenuated in mice ( $5 \times 10^8$  or  $1 \times 10^9$  PFU). Surprisingly, 84% (6/7) of the mice treated with VSV-M(mut)-mp53 compared to 14% (1/7) of the mice

TABLE 1. VSV-M(mut)-mp53 is highly attenuated *in vivo*

Virus	rVSV toxicity in BALB/c mice <sup>a</sup>			
	Dose (PFU/mouse)	Route	Mortality	% Mortality
VSV-M(mut)-mp53	$1 \times 10^8$	I.v.	0/7	0
VSV-mp53	$1 \times 10^8$	I.v.	0/7	0
VSV-M(mut)	$1 \times 10^8$	I.v.	0/7	0
VSV-GFP	$1 \times 10^8$	I.v.	1/7	14
VSV-M(mut)-mp53	$5 \times 10^8$	I.v.	0/7	0
VSV-mp53	$5 \times 10^8$	I.v.	5/7	71
VSV-M(mut)	$5 \times 10^8$	I.v.	5/7	71
VSV-M(mut)-GFP	$5 \times 10^8$	I.v.	5/7	71
VSV-GFP	$5 \times 10^8$	I.v.	7/7	100
VSV-M(mut)-mp53	$1 \times 10^9$	I.v.	1/7	14
VSV-mp53	$1 \times 10^9$	I.v.	7/7	100
VSV-M(mut)	$1 \times 10^9$	I.v.	6/7	86
VSV-M(mut)-GFP	$1 \times 10^9$	I.v.	7/7	100
VSV-GFP	$1 \times 10^9$	I.v.	7/7	100

<sup>a</sup> BALB/c mice ( $n = 7$ ) were infected i.v. with increasing doses of rVSV, and mortality was monitored. Log rank tests results were as follows: for mice treated with  $1 \times 10^8$  PFU,  $P = 0.0042$ ; for mice treated with  $5 \times 10^8$  PFU,  $P = 0.0256$ ; for mice treated with  $1 \times 10^9$  PFU,  $P = 0.0257$ .

treated with VSV-M(mut) survived infection with  $1 \times 10^9$  PFU [one died shortly after inoculation with VSV-M(mut)-mp53, but not through virus-induced encephalitis]. This experiment highlighted that mp53 expression in an M-defective VSV perhaps had an additive effect, since mice infected with VSV- $\Delta$ M or VSV-mp53 exhibited increased mortality compared to VSV-M(mut)-mp53. These data demonstrated that VSV-M(mut)-mp53 is highly attenuated and yet retains *in vitro* oncolytic activity and could thus be suitable for examination as a cancer therapeutic using *in vivo* tumor models.

To assess the antitumor efficacy of VSV-M(mut)-mp53 and VSV-mp53, we chose a BALB/c syngeneic tumor model using TS/A mammary adenocarcinoma cells stably transfected with a luciferase reporter (TS/A-luc) developed by our laboratory (17, 41). Wild-type BALB/c mice ( $n = 7$ ) were injected i.v. with  $1 \times 10^5$  TS/A-luc cells. Three days later, the mice were treated with  $5 \times 10^7$  or  $5 \times 10^8$  PFU of VSV-M(mut)-mp53, mock treated, or treated with  $5 \times 10^7$  PFU of control virus VSV-GFP, VSV-mp53, or VSV-M(mut). One advantage of TS/A-luc is that this reagent allows *in vivo* monitoring of tumor growth using an *in vivo* imaging system (IVIS). Measurement of luciferase activity can thus be used to assess the relative tumor burden. Representative images, along with luciferase signal quantification, from days 14 and 28 after tumor administration are shown for mock-, VSV-M(mut)-mp53-, and VSV-mp53-treated mice (Fig. 4A). Noticeably, luciferase activity is absent in mice treated with VSV-M(mut)-mp53 up to 28 days after tumor inoculation. This strategy, using a single dose ( $5 \times 10^7$  PFU) of VSV-M(mut)-mp53, significantly protected BALB/c mice from TS/A-luc tumor-induced death compared to similar doses of control rVSVs ( $n = 7$ ;  $P = 0.0045$ ). Mice treated with VSV-M(mut), VSV-mp53, VSV-GFP, and an increased dose ( $5 \times 10^8$  PFU) of VSV-M(mut)-mp53 had median survival times ranging from 40 to 75 days. However, less than 50% of VSV-M(mut)-mp53 mice treated with  $5 \times 10^7$  PFU succumbed over 120 days posttreatment, and thus, a mean could not be determined (Fig. 4B).

Because VSV-M(mut)-mp53 exhibited low toxicity, we also

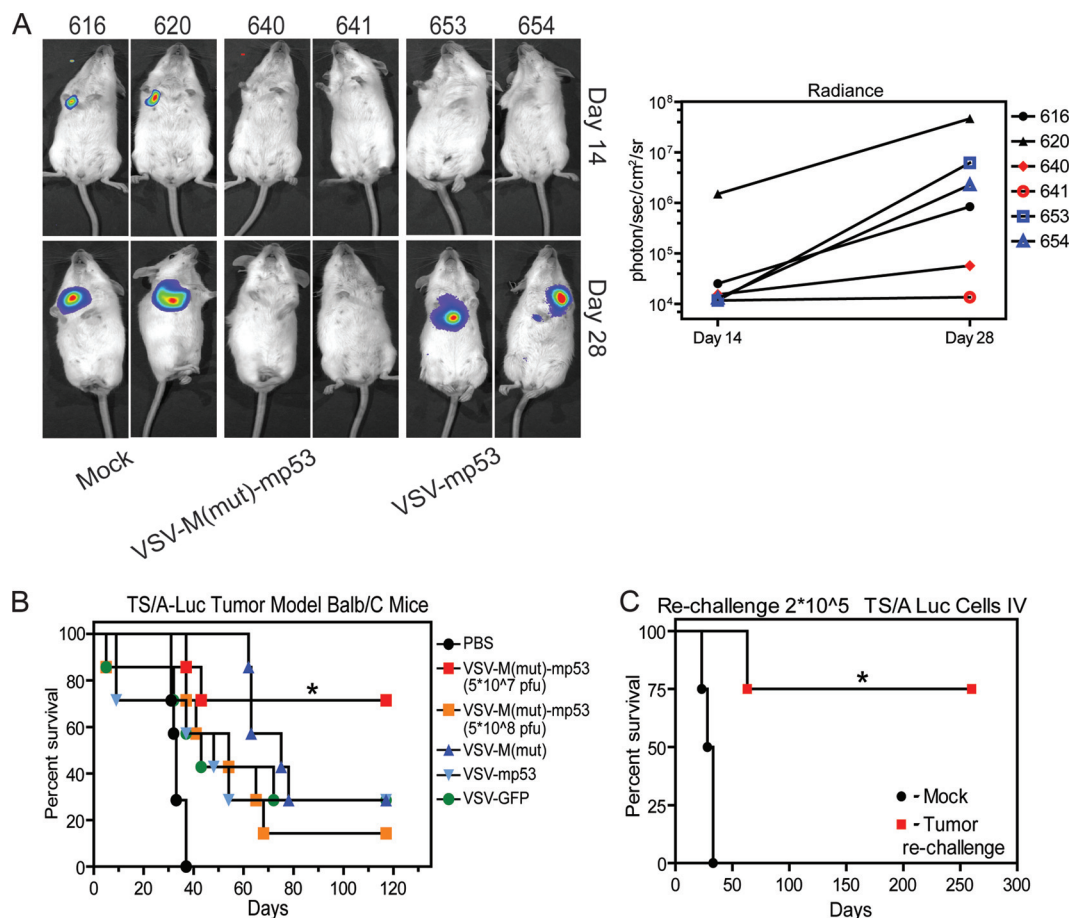


FIG. 4. VSV-M(mut)-mp53 protects immunocompetent mice from TS/A-luc formation. (A) Mock- or rVSV-treated mice were anesthetized and injected intraperitoneally (i.p.) with a luciferin substrate, and luciferase activity was detected using the IVIS. Representative images from mock-, VSV-M(mut)-mp53-, and VSV-mp53-treated mice are shown. Luciferase radiance is an indicator of tumor burden and is quantified using Living Image software (right). (B) BALB/c mice ( $n = 7$ ) were initially given  $1 \times 10^5$  TS/A-luc cells i.v. on day 0 and were then either mock or rVSV treated [ $5 \times 10^7$  PFU or  $5 \times 10^8$  PFU VSV-M(mut)-mp53 only] on day 3. The mice were then monitored for survival (\*,  $P = 0.0045$ ; log rank test). (C) Previously treated or naïve mice ( $n = 4$ ) were challenged with  $2 \times 10^5$  TS/A-luc cells on day 120 (day 0 for rechallenge), and survival was monitored (\*,  $P = 0.0091$ ; log rank test).

hypothesized that using an increased dose of agent would lead to enhanced antitumor clearance. However, treatment with  $5 \times 10^8$  PFU VSV-M(mut)-mp53 protected only 14% of animals compared to treatment at a lower dose ( $5 \times 10^7$  PFU), at which approximately 71% of mice survived (Fig. 4B). It is thus possible that the increased viral presence biases the immune response to the excess of viral antigens rather than tumor cell antigens. The stimulation of antitumor cell activity by VSV oncolytic therapy is known to greatly facilitate tumor cell clearance (44, 46). Surviving mice previously treated with VSV-M(mut)-mp53 ( $n = 4$ ) were rechallenged with  $2 \times 10^5$  TS/A-luc cells to determine if lasting immunity against the tumor was apparent. Our results indicated that immunologic memory is indeed generated against TS/A-luc by VSV-M(mut)-mp53 and that tumor clearance is likely facilitated by the host immune response, since 75% of the mice survived tumor rechallenge up to an additional 250 days until sacrifice. One of the rechallenge mice did succumb to tumor regrowth, however, likely indicating immune escape of the tumor, but only after doubling

the median survival time of the naïve mice (60 versus 30.5 days;  $P = 0.004$ ) (Fig. 4C).

**VSV-M(mut)-mp53 stimulates antitumor immunity.** Our analysis indicated that antitumor immune responses were generated by mice with TS/A treated with VSV-M(mut)-mp53 (Fig. 4C). We therefore sought to determine if VSV-M(mut)-mp53 was able to modulate the immune compartment and host antitumor responses (Fig. 5A and B). We inoculated mice ( $n = 6$ ) with VSV-M(mut)-mp53, VSV-M(mut), VSV-mp53, or VSV-GFP and measured splenic CD8<sup>+</sup> cells (Fig. 5A). We then performed an ELISPOT assay using mitomycin C-treated TS/A-luc cells as targets to determine if VSV-M(mut)-mp53 increased the number of tumor-specific IFN- $\gamma$ -secreting T cells compared to control viruses (Fig. 5B). Indeed, tumor-bearing mice that received VSV-M(mut)-mp53 had elevated numbers of tumor-specific CD8<sup>+</sup> T cells compared to controls receiving VSV-M(mut) and VSV-GFP. We then repeated the toxicity and tumor model experiments in athymic BALB/c nude mice to further establish the necessity for an intact adaptive immune

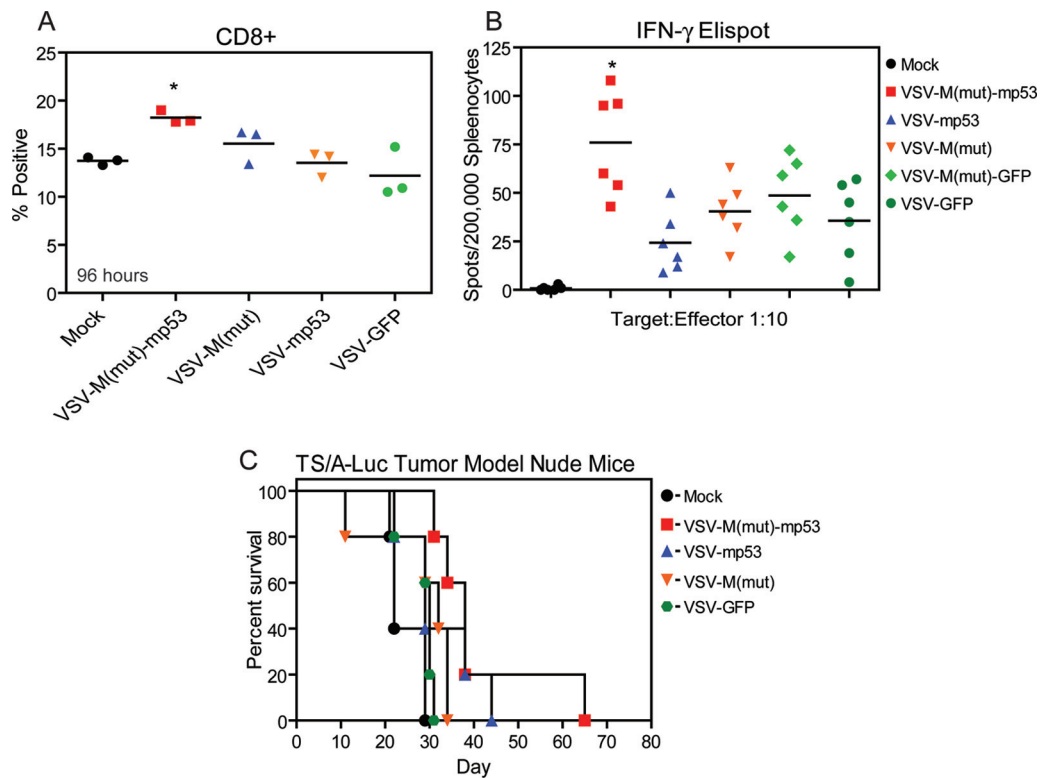


FIG. 5. VSV-M(mut)-mp53 modulates T cells and is attenuated in athymic BALB/c nude mice. (A) BALB/c mice ( $n = 3$ ) were infected with  $5 \times 10^7$  PFU rVSV; 96 h postinfection, the spleens were removed and total splenocytes were assessed for the percentage of CD8<sup>+</sup> cells by flow cytometry (\*,  $P = 0.0069$ ; one-way ANOVA). (B) BALB/c mice ( $n = 6$ ) were initially given  $1 \times 10^5$  TS/A-luc cells i.v. on day 0 and were then either mock treated or treated with  $5 \times 10^7$  PFU rVSV on day 3. On day 13, the mice were sacrificed, and total splenocytes were used for an IFN- $\gamma$  ELISPOT with mitomycin C-treated TS/A-luc cells as the target (\*,  $P < 0.0001$ ; one-way ANOVA). Horizontal lines indicate means of results. (C) Athymic BALB/c nude mice ( $n = 5$ ) were injected with  $1 \times 10^5$  TS/A-luc cells on day 0, mock treated or treated with  $5 \times 10^7$  PFU rVSV on day 3, and then observed for survival ( $P = 0.2077$ ; log rank test).

compartment for complete tumor clearance. It has previously been reported that mice lacking T cells succumb to i.v. and i.n. VSV infection at low doses approximately 3 to 4 weeks after exposure (57). To determine the role of T cell activity in p53 action, athymic BALB/c nude mice ( $n = 5$ ) were infected i.v. with  $5 \times 10^7$  PFU or i.n. with  $5 \times 10^8$  PFU VSV- $\Delta$ M-mp53, VSV-mp53, or control rVSVs, and their survival was monitored for 80 or 120 days (Table 2). Surprisingly, these mice tolerated i.v. treatment with  $5 \times 10^7$  PFU of VSV-M(mut) or

VSV-M(mut)-mp53. This analysis indicates that protection from modest i.v. doses of VSV-M(mut)-mp53 is likely due to modulation of the innate immune response, possibly involving the production of type I IFN, and not T cells. It is known that p53 can be induced by IFN signaling, can enhance IFN signaling, and can play a role in antiviral responses to VSV, since p53 knockout mice display increased susceptibility to VSV infection (39, 40, 55). Interestingly, however, all Nude mice succumbed to rVSVs following i.n. inoculation (Table 2). This may be due to rapid VSV transmission to the central nervous system (CNS) via olfactory nerve infection, resulting in increased morbidity (47). We next assessed rVSV antitumor efficacy using TS/A-luc in athymic BALB/c nude ( $n = 5$ ) mice with the treatment schedule previously described (Fig. 5C). All nude mice treated with rVSV succumbed to tumor formation, highlighting the requirement for an intact T cell compartment in eliciting protection from TS/A-luc tumor formation.

In addition to modulating CD8<sup>+</sup> T cells, it was also possible that treatment with VSV-M(mut)-mp53 could alter additional antitumor immune effector mechanisms, including cytokine profiles, in treated mice. To further elucidate the mechanisms of protection and reduced toxicity manifested by VSV-M(mut)-mp53, we sought to characterize the spleens and cytokine profiles of mice after rVSV administration (Fig. 6). In addition to CD8<sup>+</sup> T cells (Fig. 5A), the population of CD49b<sup>+</sup> cells, an

TABLE 2. VSV-M(mut)-mp53 toxicity in nude mice

Virus	rVSV Toxicity in BALB/c nude mice <sup>a</sup>			
	Dose (PFU/mouse)	Route	Mortality	% Mortality
VSV-M(mut)-mp53	$5 \times 10^7$	I.v.	0/5	0
VSV-mp53	$5 \times 10^7$	I.v.	5/5	100
VSV-M(mut)	$5 \times 10^7$	I.v.	0/5	0
VSV-GFP	$5 \times 10^7$	I.v.	3/5	60
VSV-M(mut)-mp53	$1 \times 10^9$	I.v.	3/5	60
VSV-M(mut)-mp53	$5 \times 10^8$	I.n.	5/5	100
VSV-mp53	$5 \times 10^8$	I.n.	5/5	100
VSV-M(mut)	$5 \times 10^8$	I.n.	5/5	100
VSV-GFP	$5 \times 10^8$	I.n.	5/5	100

<sup>a</sup> Athymic BALB/c nude mice ( $n = 5$ ) were infected with  $5 \times 10^7$  PFU i.v. and  $5 \times 10^8$  PFU i.n. and observed for mortality.

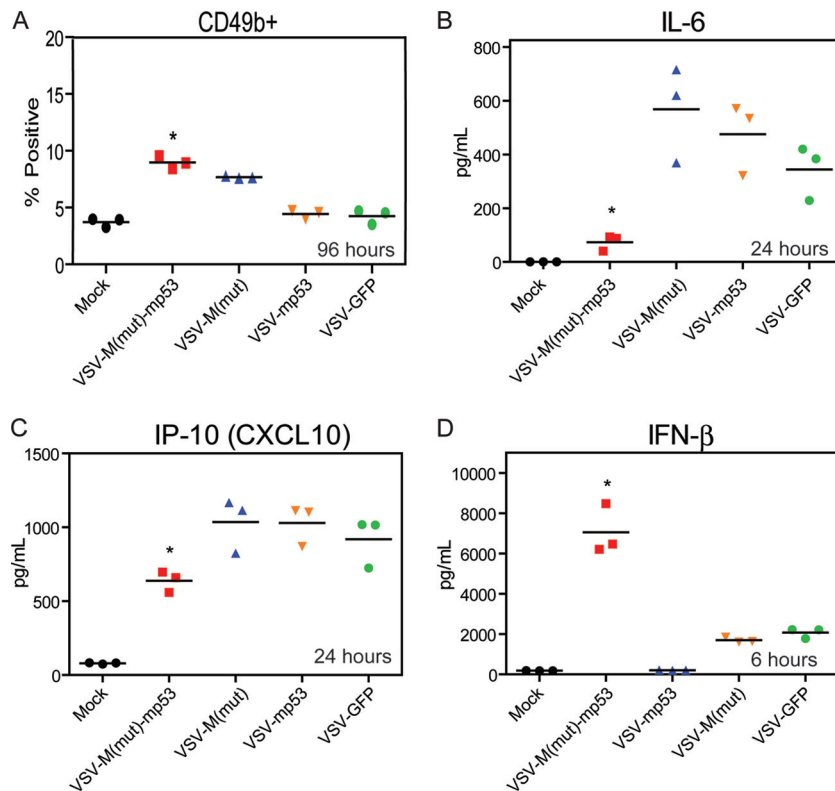


FIG. 6. VSV-M(mut)-mp53 modulates NK cell and cytokine profiles. (A, B, and C) BALB/c mice ( $n = 6$ ) were treated with  $5 \times 10^7$  PFU rVSV i.v.; 24 and 96 h postinfection, splenocytes and sera were collected. (A) The splenocytes were stained for flow cytometry to determine the number that were CD49b<sup>+</sup> (\*,  $P < 0.0001$ ; one-way ANOVA). (B and C) Sera were used for a multiplex ELISA in which IL-6 (B) and IP-10 (C) showed significant differences (\*,  $P < 0.0001$ ; one-way ANOVA). (D) BALB/c mice ( $n = 3$ ) were infected with  $5 \times 10^7$  PFU rVSV. Six hours postinfection, sera were collected, and ELISA was used to assess IFN- $\beta$  (\*,  $P = 0.0003$ ; one-way ANOVA). Horizontal lines indicate means of results.

NK cell marker, also increased in the spleens of mice infected with VSV-M(mut)-mp53 96 h postinfection (Fig. 6A). Serum cytokine levels were then tested using multiplex and IFN- $\beta$  ELISAs. Treatment with VSV- $\Delta$ M-mp53 or control rVSVs led to the expected increases in antiviral-induced cytokines, such as tumor necrosis factor alpha (TNF- $\alpha$ ) and RANTES (references 30 and 31 and data not shown). However, treatment with VSV-M(mut)-mp53 appeared to blunt the production of inflammatory cytokines, such as interleukin 6 (IL-6) and IP-10, since reduced levels were observed in VSV-M(mut)-mp53-infected mouse serum (Fig. 6B and C). IL-6 has been shown to facilitate angiogenesis and tumor cell growth, indicating that its suppression may benefit tumor clearance (2, 8). IP-10 is a proinflammatory chemoattractant that induces immune cell infiltration in response to viral infection and may have antitumor effects in some situations (4, 14, 43). Moderated levels of IP-10 may allow a more optimal antitumor response to occur and mitigate some infiltration of immune cells, possibly reducing CNS toxicity. Furthermore, VSV- $\Delta$ M-mp53 significantly increased the amount of IFN- $\beta$  present in the serum 6 h postinfection (Fig. 6D). The cytokine profiles in these mice may begin to explain the reduced toxicity displayed by VSV-M(mut)-mp53, for example, by limiting inflammatory responses and increasing IFN- $\beta$  production, which could limit virus spread as well as facilitate increased tumor clearance.

## DISCUSSION

A variety of recombinant VSVs have been developed as therapeutic agents to treat cancer (17, 18, 44, 46). This has been done by generating viruses harboring mutated VSV proteins [VSV-M(mut)] and/or inserting transgenes that modulate the innate and adaptive immune responses. Here, our data clearly demonstrate that the insertion of mp53 into the VSV-M(mut) background produces a highly attenuated and effective rVSV. It is well known that rVSV preferentially replicates in and kills transformed cells *in vitro* and *in vivo*, and VSV-M(mut)-mp53 retains this ability (11). Furthermore, the mp53 transgene appears functional and is at least phosphorylated on serines 18 and 389. As described above, phosphorylation on serine 18 enables dissociation of mp53 from MDM-2, an E3 ubiquitin ligase that negatively regulates mp53 by targeting it for proteasomal degradation. Phosphorylation on serine 389 allows oligomerization and DNA binding to occur, which are necessary steps for transcription activation of p53 (21, 27, 37, 51). Phosphorylated mp53 expressed from rVSV activated a luciferase reporter gene under the control of a p53-responsive promoter more potently when expressed from the VSV-M(mut) background. This included clearly enhanced expression of MDM-2 and p21 mRNAs, which are known mp53 targets. The tumor suppressor p53 has the ability to exert many effects when

transcriptionally active in cells. For example, p53 reactivation in hepatocellular carcinoma led to the induction of innate immune signaling and to tumor regression (62). It has also been reported that p53 can cross talk with the IFN system and plays an essential role in antiviral immunity (40, 55). IFN-inducible ISGF3 can activate the transcription of p53, and TLR3 production can be initiated by p53 (56). Additionally, IFN treatment can activate apoptotic pathways in both p53-dependent and -independent manners (22, 29, 64). Interestingly, mice that have an extra copy of the p53 gene ("super p53" mice) are remarkably resistant to VSV infection, whereas p53 knockout mice are highly susceptible to infection, again highlighting the potential role of p53 in antiviral immunity (39, 40). Furthermore, p53 is known to regulate the cell cycle, apoptosis, microRNAs (miRNAs), and senescence, all of which could have a benefit when expressed from VSV-M(mut)-mp53 in the tumor microenvironment (10, 12, 28, 54).

VSV-M(mut)-mp53 was highly attenuated *in vivo* and showed potent ability to clear metastatic disease from immunocompetent BALB/c mice. The reduced toxicity associated with the virus allowed administration of 20 times more virus without significant mortality. However, increasing the treatment dose 10-fold to  $5 \times 10^8$  PFU did not increase VSV-M(mut)-mp53 antitumor efficacy. It is possible that by increasing the viral load the secondary immune response becomes more heavily focused on viral antigens and cannot respond efficiently to tumor cell antigens due to being overwhelmed. Furthermore, it is possible that infection at higher doses may lead to an increase in regulatory T cells or myeloid-derived suppressor cells (MDSC), which could dampen the antitumor response. Surprisingly, VSV-M(mut)-mp53 appears attenuated in athymic BALB/c nude mice following i.v. inoculation, indicating that viral clearance is not completely dependent on T cells and that VSV-M(mut)-mp53 likely modulates the innate immune response in order to control viral infection.

It has previously been shown that oncolytic virotherapy using VSV, as well as other viruses, can lead to cross-presentation of tumor antigens and induction of a host antitumor response (7, 18, 60). We therefore determined whether VSV-M(mut)-mp53 treatment might modulate components of the innate and adaptive immune systems in order to elicit a cross-presentation response and facilitate tumor clearance. Indeed, mice treated with VSV-M(mut)-mp53 showed increased numbers of tumor-specific CD8<sup>+</sup> T cells and CD49b<sup>+</sup> NK cells in the spleen 96 h postinfection. Increasing the number of CD49b<sup>+</sup> NK cells is advantageous, as these cells have cytolytic abilities and can directly kill virus-infected tumor cells. This also leads to the production of tumor cell debris, which can be processed and displayed by antigen-presenting cells, leading to the generation of tumor-specific CD8<sup>+</sup> T cells that can enhance tumor protection (24). It is thus not surprising that athymic BALB/c nude mice were not protected from TS/A-luc tumor formation, since these mice lack T cells.

As mentioned above, VSV-M(mut)-mp53 was found to modulate the cell population in the spleen, as exhibited by CD49b<sup>+</sup> cells. VSV-M(mut)-mp53 also affected the serum levels of cytokines and chemokines in infected animals. Normally, viral infection leads to production of inflammatory and antiviral cytokines and chemokines, like IL-6, IP-10, TNF- $\alpha$ , and

IFN- $\beta$ . However, treatment with high doses of rVSV can lead to increased expression of these molecules, which can cause lethality by inducing a fatal cytokine storm (25). Our data indicated that VSV-M(mut)-mp53 administration led to a reduction in the serum levels of IL-6 and IP-10 24 h after treatment while serum IFN- $\beta$  levels were elevated 6 h postinfection. mp53 has been reported to be a potential negative regulator of IL-6 and suppressor of macrophage activation (2, 32, 50). IL-6 can act as a proinflammatory cytokine that signals through the IL-6 $\alpha$ -gp130 receptor complex and activates JAKs, which in turn activate a number of STAT molecules (23). IL-6 is also the primary mediator of the acute-phase fever response and could be a component of inflammatory responses seen with increased doses of rVSV (19). IP-10 (CXCL10) levels were also reduced in the sera of VSV-M(mut)-mp53-treated mice. IP-10 is a proinflammatory chemokine that functions as a chemoattractant for macrophages, dendritic cells (DC), and NK cells by binding to CXCR3 (3, 14). The reduction in serum IP-10 may reduce immune cell infiltration into sites where the furtherance of inflammation may be deleterious to the host. Furthermore, the decreased inflammation associated with VSV-M(mut)-mp53 could allow a more finely tuned antitumor response to occur by not biasing the immune response against the viral infection. Thus, it is possible that a reduction in the expression of IL-6 and IP-10, along with the suppression of macrophage activation in the presence of increased levels of IFN- $\beta$ , may facilitate a reduction in VSV-M(mut)-mp53 toxicity and enhance antitumor efficacy. However, it is also important to note that the innate immune system can have disparate effects on oncolytic viruses. For example, rVSV has been combined with pretreatment histone deacetylase inhibitors, which can effectively blunt the antiviral response and facilitate increased tumor oncolysis (42). It has also been observed that the innate immune response can have negative impacts on the effects of other oncolytic viruses (20). Therefore, our results may be limited to the VSV-M(mut)-mp53 construct and the model systems used. Nevertheless, our data indicate that VSV-M(mut)-mp53 is a potent oncolytic vector with enhanced safety and efficacy. Thus, VSV-M(mut)-mp53 could be considered for further studies to examine the potential of this therapy as a future anticancer treatment.

#### ACKNOWLEDGMENTS

We thank Rachel Elsby, Hiroki Ishikawa, Ai Harashima, Shannon Opiela, Andrea Echeverry, and the DVR for technical assistance.

Financial support was provided by NIH grant 2-R01-CA-095924-06.

#### REFERENCES

- Adkins, B., Y. Bu, E. Cepero, and R. Perez. 2000. Exclusive Th2 primary effector function in spleens but mixed Th1/Th2 function in lymph nodes of murine neonates. *J. Immunol.* **164**:2347–2353.
- Angelo, L. S., M. Talpaz, and R. Kurzrock. 2002. Autocrine interleukin-6 production in renal cell carcinoma: evidence for the involvement of p53. *Cancer Res.* **62**:932–940.
- Angiolillo, A. L., et al. 1995. Human interferon-inducible protein 10 is a potent inhibitor of angiogenesis *in vivo*. *J. Exp. Med.* **182**:155–162.
- Arai, K., Z. X. Liu, T. Lane, and G. Dennert. 2002. IP-10 and Mig facilitate accumulation of T cells in the virus-infected liver. *Cell Immunol.* **219**:48–56.
- Balachandran, S., and G. N. Barber. 2004. Defective translational control facilitates vesicular stomatitis virus oncolysis. *Cancer Cell* **5**:51–65.
- Balachandran, S., et al. 1998. Activation of the dsRNA-dependent protein kinase, PKR, induces apoptosis through FADD-mediated death signaling. *EMBO J.* **17**:6888–6902.
- Boudreau, J. E., et al. 2011. IL-15 and type I interferon are required for

- activation of tumoricidal NK cells by virus-infected dendritic cells. *Cancer Res.* **71**:2497–2506.
8. **Bromberg, J., and T. C. Wang.** 2009. Inflammation and cancer: IL-6 and STAT3 complete the link. *Cancer Cell* **15**:79–80.
  9. **Brooks, C. L., and W. Gu.** 2003. Ubiquitination, phosphorylation and acetylation: the molecular basis for p53 regulation. *Curr. Opin. Cell Biol.* **15**:164–171.
  10. **Caelles, C., A. Helmborg, and M. Karin.** 1994. p53-dependent apoptosis in the absence of transcriptional activation of p53-target genes. *Nature* **370**:220–223.
  11. **Capo-chichi, C. D., et al.** 2010. Explicit targeting of transformed cells by VSV in ovarian epithelial tumor-bearing Wv mouse models. *Gynecol. Oncol.* **116**:269–275.
  12. **Chipuk, J. E., and D. R. Green.** 2006. Dissecting p53-dependent apoptosis. *Cell Death Differ.* **13**:994–1002.
  13. **Cuddihy, A. R., A. H. Wong, N. W. Tam, S. Li, and A. E. Koromilas.** 1999. The double-stranded RNA activated protein kinase PKR physically associates with the tumor suppressor p53 protein and phosphorylates human p53 on serine 392 in vitro. *Oncogene* **18**:2690–2702.
  14. **Dufour, J. H., et al.** 2002. IFN-gamma-inducible protein 10 (IP-10; CXCL10)-deficient mice reveal a role for IP-10 in effector T cell generation and trafficking. *J. Immunol.* **168**:3195–3204.
  15. **Enninga, J., D. E. Levy, G. Blobel, and B. M. A. Fontoura.** 2002. Role of nucleoporin induction in releasing an mRNA nuclear export block. *Science* **295**:1523–1525.
  16. **Faria, P. A., et al.** 2005. VSV disrupts the Rae1/mrnp41 mRNA nuclear export pathway. *Mol. Cell* **17**:93–102.
  17. **Fernandez, M., M. Porosnicu, D. Markovic, and G. N. Barber.** 2002. Genetically engineered vesicular stomatitis virus in gene therapy: application for treatment of malignant disease. *J. Virol.* **76**:895–904.
  18. **Galivo, F., et al.** 2010. Single-cycle viral gene expression, rather than progressive replication and oncolysis, is required for VSV therapy of B16 melanoma. *Gene Ther.* **17**:158–170.
  19. **Gervois, P., et al.** 2004. Global suppression of IL-6-induced acute phase response gene expression after chronic in vivo treatment with the peroxisome proliferator-activated receptor- $\alpha$  activator fenofibrate. *J. Biol. Chem.* **279**:16154–16160.
  20. **Guo, Z. S., S. H. Thorne, and D. L. Bartlett.** 2008. Oncolytic virotherapy: molecular targets in tumor-selective replication and carrier cell-mediated delivery of oncolytic viruses. *Biochim. Biophys. Acta* **1785**:217–231.
  21. **Hao, M., et al.** 1996. Mutation of phosphoserine 389 affects p53 function in vivo. *J. Biol. Chem.* **271**:29380–29385.
  22. **He, L., et al.** 2007. A microRNA component of the p53 tumour suppressor network. *Nature* **447**:1130–1134.
  23. **Heinrich, P. C., I. Behrmann, G. Müller-Newen, F. Schaper, and L. Graeve.** 1998. Interleukin-6-type cytokine signalling through the gp130/Jak/STAT pathway. *Biochem. J.* **334**:297–314.
  24. **Hinrichs, C., et al.** 2009. Adoptively transferred effector cells derived from naive rather than central memory CD8<sup>+</sup> T cells mediate superior antitumor immunity. *Proc. Natl. Acad. Sci. U. S. A.* **106**:17469–17474.
  25. **Hod, E. A., et al.** 2008. Cytokine storm in a mouse model of IgG-mediated hemolytic transfusion reactions. *Blood* **112**:891–894.
  26. **Horvath, M. M., X. Wang, M. A. Resnick, and D. A. Bell.** 2007. Divergent evolution of human p53 binding sites: cell cycle versus apoptosis. *PLoS Genet.* **3**:e127.
  27. **Huang, C., W. Y. Ma, A. Maxiner, Y. Sun, and Z. Dong.** 1999. p38 kinase mediates UV-induced phosphorylation of p53 protein at serine 389. *J. Biol. Chem.* **274**:12229–12235.
  28. **Hussain, S. P., and C. C. Harris.** 2006. p53 biological network: at the crossroads of the cellular-stress response pathway and molecular carcinogenesis. *J. Nippon Med. Sch.* **73**:54–64.
  29. **Kannan, K., et al.** 2001. DNA microarrays identification of primary and secondary target genes regulated by p53. *Oncogene* **20**:2225–2234.
  30. **Kato, H., et al.** 2005. Cell type-specific involvement of RIG-I in antiviral response. *Immunity* **23**:19–28.
  31. **Kawai, T., et al.** 2005. IPS-1, an adaptor triggering RIG-I- and Mda5-mediated type I interferon induction. *Nat. Immunol.* **6**:981–988.
  32. **Komarova, E. A., et al.** 2005. p53 is a suppressor of inflammatory response in mice. *FASEB J.* **19**:1030–1032.
  33. **Kruse, J., and W. Gu.** 2009. Modes of p53 regulation. *Cell* **137**:609–622.
  34. **Lawson, N. D., E. A. Stillman, M. A. Whitt, and J. K. Rose.** 1995. Recombinant vesicular stomatitis viruses from DNA. *Proc. Natl. Acad. Sci. U. S. A.* **92**:4477–4481.
  35. **Li, H., K.-W. Peng, D. Dingli, R. A. Kratzke, and S. J. Russell.** 2010. Oncolytic measles viruses encoding interferon beta and the thyroidal sodium iodide symporter gene for mesothelioma virotherapy. *Cancer Gene Ther.* **17**:550–558.
  36. **Meek, D. W.** 1999. Mechanisms of switching on p53: a role for covalent modification? *Oncogene* **18**:7666–7675.
  37. **Meek, D. W.** 1998. Multisite phosphorylation and the integration of stress signals at p53. *Cell Signal.* **10**:159–166.
  38. **Melchior, F., and L. Hengst.** 2002. SUMO-1 and p53. *Cell Cycle* **1**:245–249.
  39. **Munoz-Fontela, C., et al.** 2005. Resistance to viral infection of super p53 mice. *Oncogene* **24**:3059–3062.
  40. **Munoz-Fontela, C., et al.** 2008. Transcriptional role of p53 in interferon-mediated antiviral immunity. *J. Exp. Med.* **205**:1929–1938.
  41. **Nanni, P., C. de Giovanni, P. L. Lollini, G. Nicoletti, and G. Prodi.** 1983. TS/A: a new metastasizing cell line from a BALB/c spontaneous mammary adenocarcinoma. *Clin. Exp. Metastasis* **1**:373–380.
  42. **Nguyen, T. L.-A., et al.** 2008. Chemical targeting of the innate antiviral response by histone deacetylase inhibitors renders refractory cancers sensitive to viral oncolysis. *Proc. Natl. Acad. Sci. U. S. A.* **105**:14981–14986.
  43. **Nie, C. Q., et al.** 2009. IP-10-mediated T cell homing promotes cerebral inflammation over splenic immunity to malaria infection. *PLoS Pathog.* **5**:e1000369.
  44. **Obuchi, M., M. Fernandez, and G. N. Barber.** 2003. Development of recombinant vesicular stomatitis viruses that exploit defects in host defense to augment specific oncolytic activity. *J. Virol.* **77**:8843–8856.
  45. **Porosnicu, M., A. Mian, and G. N. Barber.** 2003. The oncolytic effect of recombinant vesicular stomatitis virus is enhanced by expression of the fusion cytosine deaminase/uracil phosphoribosyltransferase suicide gene. *Cancer Res.* **63**:8366–8376.
  46. **Ramsburg, E., et al.** 2005. A vesicular stomatitis virus recombinant expressing granulocyte-macrophage colony-stimulating factor induces enhanced T-cell responses and is highly attenuated for replication in animals. *J. Virol.* **79**:15043–15053.
  47. **Reiss, C. S., I. V. Plakhov, and T. Komatsu.** 1998. Viral replication in olfactory receptor neurons and entry into the olfactory bulb and brain. *Ann. N. Y. Acad. Sci.* **855**:751–761.
  48. **Roberts, M. S., R. M. Lorence, W. S. Groene, and M. K. Bamat.** 2006. Naturally oncolytic viruses. *Curr. Opin. Mol. Ther.* **8**:314–321.
  49. **Saloura, V., et al.** 2010. Evaluation of an attenuated vesicular stomatitis virus vector expressing interferon-beta for use in malignant pleural mesothelioma: heterogeneity in interferon responsiveness defines potential efficacy. *Hum. Gene Ther.* **21**:51–64.
  50. **Santhanam, U., A. Ray, and P. B. Sehgal.** 1991. Repression of the interleukin 6 gene promoter by p53 and the retinoblastoma susceptibility gene product. *Proc. Natl. Acad. Sci. U. S. A.* **88**:7605–7609.
  51. **She, Q. B., N. Chen, and Z. Dong.** 2000. ERKs and p38 kinase phosphorylate p53 protein at serine 15 in response to UV radiation. *J. Biol. Chem.* **275**:20444–20449.
  52. **Shieh, S. Y., M. Ikeda, Y. Taya, and C. Prives.** 1997. DNA damage-induced phosphorylation of p53 alleviates inhibition by MDM2. *Cell* **91**:325–334.
  53. **Shio, Y., T. Yamamoto, and N. Yamaguchi.** 1992. Negative regulation of Rb expression by the p53 gene product. *Proc. Natl. Acad. Sci. U. S. A.* **89**:5206–5210.
  54. **Suzuki, H. I., et al.** 2009. Modulation of microRNA processing by p53. *Nature* **460**:529–533.
  55. **Takaoka, A., et al.** 2003. Integration of interferon-alpha/beta signalling to p53 responses in tumour suppression and antiviral defence. *Nature* **424**:516–523.
  56. **Taura, M., et al.** 2008. p53 regulates Toll-like receptor 3 expression and function in human epithelial cell lines. *Mol. Cell. Biol.* **28**:6557–6567.
  57. **Thomsen, A. R., et al.** 1997. Cooperation of B cells and T cells is required for survival of mice infected with vesicular stomatitis virus. *Int. Immunol.* **9**:1757–1766.
  58. **Venkataraman, T., et al.** 2007. Loss of DEX/H box RNA helicase LGP2 manifests disparate antiviral responses. *J. Immunol.* **178**:6444–6455.
  59. **von Kobbe, C., et al.** 2000. Vesicular stomatitis virus matrix protein inhibits host cell gene expression by targeting the nucleoporin Nup98. *Mol. Cell* **6**:1243–1252.
  60. **Wongthida, P., et al.** 2011. Activating systemic T cell immunity against self tumor antigens to support oncolytic virotherapy with VSV. *Hum. Gene Ther.* doi:10.1089/hum.2010.216.
  61. **Wu, L., et al.** 2008. rVSV(M Delta 51)-M3 is an effective and safe oncolytic virus for cancer therapy. *Hum. Gene Ther.* **19**:635–647.
  62. **Xue, W., et al.** 2007. Senescence and tumour clearance is triggered by p53 restoration in murine liver carcinomas. *Nature* **445**:656–660.
  63. **Yang, Q., et al.** 2010. Pharmacological inhibition of BMK1 suppresses tumor growth through promyelocytic leukemia protein. *Cancer Cell* **18**:258–267.
  64. **Zhang, F., and S. Sriram.** 2009. Identification and characterization of the interferon-beta-mediated p53 signal pathway in human peripheral blood mononuclear cells. *Immunology* **128**:e905–e918.